

Isoforms of the orphan nuclear receptor COUP-TFII differentially modulate pancreatic cancer progression

SIMONE POLVANI¹, SARA PEPE^{2,3}, SARA TEMPESTI¹, MIRKO TAROCCHI¹, GIADA MARRONCINI⁴,
LAPO BENCINI⁵, ELISABETTA CENI¹, TOMMASO MELLO¹, LUCIA PICARIELLO¹,
IRENE SIMEONE^{1,3}, CECILIA GRAPPONE¹, GABRIELE DRAGONI¹, LORENZO ANTONUZZO⁶,
ELISA GIOMMONI⁷, STEFANO MILANI¹ and ANDREA GALLI¹

¹Gastroenterology Research Unit, Department of Experimental and Clinical Biomedical Sciences ‘Mario Serio’, University of Florence, I-50134 Florence; ²Core Research Laboratory, Institute for Cancer Research and Prevention, I-50139 Florence; ³Department of Medical Biotechnologies, University of Siena, I-53100 Siena; ⁴Endocrinology Research Unit, Department of Experimental and Clinical Biomedical Sciences ‘Mario Serio’, University of Florence; ⁵Oncology General Surgery, Azienda Ospedaliero Universitaria Careggi; ⁶Department of Experimental and Clinical Medicine, University of Florence; ⁷Medical Oncology, Azienda Ospedaliero Universitaria Careggi, I-50139 Florence, Italy

Received September 8, 2021; Accepted February 7, 2022

DOI: 10.3892/ijo.2022.5345

Abstract. The expression of the nuclear receptor transcription factor (TF) COUP-TFII is broadly associated with cell differentiation and cancer development, including of pancreatic ductal adenocarcinoma (PDAC), a devastating disease with one of the poorest prognoses among cancers worldwide. Recent studies have started to investigate the pathological and physiological roles of a novel COUP-TFII isoform (COUP-TFII_V2) that lacks the DNA-binding domain. As the role of the canonical COUP-TFII in PDAC was previously demonstrated, the present study evaluated whether COUP-TFII_V2 may have a functional role in PDAC. It was demonstrated that COUP-TFII_V2 naturally occurs in PDAC cells and in primary samples, where its expression is consistent with shorter overall survival and peripheral invasion. Of note, COUP-TFII_V2, exhibiting nuclear and cytosolic expression, is linked to epithelial to mesenchymal transition (EMT) and cancer progression, as confirmed by nude mouse experiments. The present results demonstrated that COUP-TFII_V2 distinctively regulates the EMT of PDAC and, similarly to its sibling, it is associated with tumor aggressiveness. The two isoforms have both overlapping and exclusive functions that cooperate with cancer growth and dissemination. By studying how PDAC cells switch from one isoform to the other, novel insight into cancer biology was

gained, indicating that this receptor may serve as a novel possible target for PDAC management.

Introduction

Pancreatic ductal adenocarcinoma (PDAC) is a deadly disease with a poor prognosis and the fourth most common cause of cancer-associated death in developed countries (1-3). Despite the indisputable progress in elucidating its pathology and mechanisms, the acquired knowledge has always been minimally translated into successful cancer treatments.

Given the importance of the interaction between cancer cells and the surrounding environment, PDAC progression may be sketched out as a combination of a series of phenomena ranging from tumor stemness, epithelial-mesenchymal transition (EMT), secretion of autocrine and paracrine factors and finally to the modification of the metabolic machinery. These aspects are tightly intertwined. On one hand, EMT is necessary for tumor spreading, acquisition of chemoresistance and mitochondrial dysfunction (4); on the other hand, the presence of cancer stem cells is associated with tumor spreading, relapse and EMT, suggesting that both EMT and stemness are strictly related events in tumor progression.

The orphan nuclear receptor transcription factor chicken ovalbumin upstream promoter transcription factor II (COUP-TFII), also known as nuclear receptor 2 family 2 (NR2F2), belongs to the orphan nuclear receptor family and has an important role in cell fate determination, neuronal and vascular organogenesis and stemness (5-11). Alterations of COUP-TFII expression and transcription activity are associated with epithelial cancer progression (12-18); furthermore, its contribution to the development of PDAC was recently highlighted (18). The role of COUP-TFII in cancer is complex: It acts both as an oncogene and as a tumor suppressor by controlling different pathways, such as angiogenesis, TGFβ signaling, telomere lengthening and cancer metabolism. The

Correspondence to: Professor Andrea Galli, Gastroenterology Research Unit, Department of Experimental and Clinical Biomedical Sciences ‘Mario Serio’, University of Florence, Viale Pieraccini 6, I-50134 Florence, Italy
E-mail: andrea.galli@unifi.it

Key words: COUP-TFII, stem cell, cancer, nuclear receptor, epithelial to mesenchymal transition

evidence that COUP-TFII deletion has little impact on adult physiological functions indicates that this receptor may be a potential therapeutic target in oncology (19).

COUP-TFII is prototyped by the steroid hormone receptor; however, it has been recently demonstrated that different COUP-TFII variants are expressed in epithelial cells and one of these variants, COUP-TFII_V2, lacks the DNA-binding domain (DBD) (10,20). Although the absence of DBD suggests a lack of transcription activity, the role of this receptor has remained elusive.

To the best of our knowledge, the involvement of COUP-TFII_V2 in cancer biology has not been previously reported; therefore, the present study was performed to elucidate the role of this recently discovered variant in the complex scenario of PDAC progression, indicating its crucial implication in cancer invasiveness and chemoresistance.

Materials and methods

Cell culture, transfection and commercially available plasmids. Pancreatic cell lines (PANC-1, BxPC3, CAPAN-2, MiaPaca2, hTERT-HPNE, PL-45 and Su.86.86) were obtained from the American Tissue Type Collection and cultured as previously described (18). Specifically, PANC-1, MiaPaca2, CAPAN-2 and PL-45 were cultured in DMEM high glucose (MilliporeSigma) with 10% Fetal Bovine Serum (FBS; Euroclone); Su.86.86 and BxPC3 cells were cultured in RPMI-1640 (MilliporeSigma)/10% FBS; hTERT-HPNE were cultured in 75% DMEM (MilliporeSigma) (with 2 mM L-glu and 1.5 g/l sodium bicarbonate, both from MilliporeSigma)/25% Medium M3 Base (Incell Corp.) with 5% FBS, 10 ng/ml human recombinant EGF (Thermo Fisher Scientific, Inc.), 5.5 mM D-glucose (1 g/l; MilliporeSigma) and 750 ng/ml puromycin (Thermo Fisher Scientific, Inc.). The transfections of plasmids were performed with FuGENE HD (Promega Corporation) according to the manufacturer's protocol. Short hairpin (sh)RNA for COUP-TFII (shNR2F2) and negative control shRNA (shNEG) are described in (18); shNR2F2 covers the same target sequence of a small interfering (si)RNA for COUP-TFII (Hs_NR2F2_6, cat. no. s103649065; Qiagen GmbH). COUP-TFII_V2-GFP (cat. no. RG226609) and COUP-TFII_V2 (cat. no. 4453629) plasmids were from OriGene Technologies, Inc.

EGFP-COUP-TFII_V1 plasmid. To produce the N-terminal enhanced green fluorescence protein (EGFP)-tagged COUP-TFII_V1 a 1.5 Kb *EcoRI/XhoI* fragment of the COUP-TFII_V1 cDNA was amplified from the plasmid pCR3.1-COUP-TFII by PCR with PFU Ultra II (Agilent Technologies) using the following primers: Forward, 5'-C AT GAATTCGGCAATGGTAG-3' and reverse, 5'-TAGAAG GCACAGTCGAGG-3'. Thermocycling conditions were as per the manufacturer's instructions with annealing at 54°C for 30 sec and extension at 72°C for 30 sec (x35 cycles); reaction mixtures were prepared as per the manufacturer's protocol. After digestion with *EcoRI* and *XhoI* enzymes (New England Biolabs, Inc.) and gel purification of the PCR product, the COUP-TFII cDNA was ligated in the *EcoRI/SalI* sites of pEGFP-C1 (GenBank accession no. U55763; cat. no. 6084-1; Clontech). The absence of errors due to PCR amplification

was confirmed by standard Sanger DNA sequencing. The pCR3.1-COUP-TFII plasmid was a kind gift of Professor M. Vasseur-Cognet [INSERM, U1016; Department of Endocrinology, Metabolism and Cancer, Cochin Institute, CNRS (UMR 8104), Paris, France].

COUP-TFII_V2-NLS plasmid. COUP-TFII_V2 was fused at the C-terminal end with a nuclear localization signal derived from SV40 virus (-PKKKRKV-) to force nuclear localization. In brief, an *EcoRI/MluI* COUP-TFII fragment, obtained by double enzymatic digestion with *EcoRI* and *MluI* (New England Biolabs, Inc) from plasmid RG226609 (OriGene Technologies, Inc.), was cloned between the *EcoRI* and *XhoI* sites of the pcDNA3.1 plasmid (cat. no. V79020; Thermo Fisher Scientific, Inc.) and the nuclear localization signal (NLS) was inserted in frame as a double-strand (ds) DNA in the *MluI/XhoI* restriction sites. Tag presence was detected by restriction digestion with the newly inserted *SpeI* site and confirmed by standard Sanger DNA sequencing. For COUP-TFII_V2NLS-EGFP, the ds oligo corresponding to the NLS was directly cloned in the *MluI/XhoI* restriction sites of the plasmid RG226609. The NLS was obtained by annealing the oligos NLS-[forward (for)/reverse (rev)] for V2-NLS and NLS-GFP (for/rev) for V2-NLS-GFP (Table SI).

Time-lapse experiment. Time-lapse experiments were performed on a Leica AM600 inverted microscope equipped with a microscope miniculture incubator (CTI-control 3400 digital) and Temp control (37-2 digital), both from Leica Microsystems GmbH. Transfected cells were plated on 35-mm μ -Dishes (Ibidi GmbH) for observation; usually, cells were followed for 16 h and images were acquired every 5 min. The average speed and linearity were measured with Icy v.2.0.3 (icy.bioimageanalysis.org).

Cell viability, apoptosis, mitochondrial membrane potential and cell senescence. Cell viability, apoptosis and mitochondrial potential were evaluated with the 'Cell Count and Viability', with the 'Annexin V & Cell Death kit' and with the 'MitoPotential kit', respectively, on a Guava Muse cell Analyzer (Luminex Corporation) following the manufacturer's protocols. Cellular senescence was histochemically determined with the Senescence detection kit (BioVision) as percentage of senescence-associated β -gal expressing cells.

Wound healing and invasiveness. A wound-healing assay was performed by plating PANC-1 clones in the chambers of μ -Dish culture inserts (Ibidi GmbH) for live cell analysis. After reaching confluence, the inserts were removed and images of the same areas were acquired immediately (time 0) and then after 4, 24 and 48 h. Captured images were then analyzed with ImageJ 1.52r inside Icy 2.0.3. To measure the wound width, its margins were determined by thresholding the images and then a straight vertical line was drawn for each margin; the wound gap was then measured as the distance between these two lines. Chemo-invasiveness was performed as described previously (18). In brief, cells suspended in serum-free medium were loaded in the top chambers of 12 multiwell Boyden chambers (Neuro Probe Inc.) at 10^4 cells/filter and complete medium was added to the lower chamber as a chemo-attractant. Upper and

Table I. COUP-TFII-V2 expression in primary samples.

Item	n	COUP-TFII_V2 relative quantities, mean (min; max); median	P-value
Sex			0.988
Male	16	1.02 (0.001; 11.2); 0.048	
Female	22	14.5 (0.002; 313); 0.039	
Age, years			0.895
<70	18	17.7 (0.001; 313); 0.03	
≥70	20	0.792 (0.002; 11.2); 0.055	
T-stage			0.247
1	1	0.002	
2	12	27.1 (0.002; 313); 0.059;	
3	24	0.415 (0.001; 4.26); 0.028	
Nodal status			0.028
N0	8	0.0238 (0.002; 0.099); 0.011	
N+	30	11.2 (0.001; 313); 0.06	
Differentiation			0.008
Low	6	0.008 (0.001; 0.014); 0.008	0.014 vs. medium
Moderate	29	11.6 (0.002; 313); 0.06	
High	3	0.016 (0.002; 0.039); 0.006	

The reported values are relative mRNA quantities normalized to GAPDH and RPL13A. TF, transcription factor.

lower chambers were separated by an 8 μ m pore polycarbonate membrane, coated with Matrigel® (Biomap snc). After 6 h of incubation at 37°C with 5% CO₂, the Boyden chambers were disassembled, the cells were removed from the upper side of the membranes with a cotton bud, the filters stained with Diff-Quick stain (Biomap snc) according to manufacturer's protocol and the cells that had transgressed to the lower surface were counted with a Leica DM4000B Microscope (Leica Microsystems GmbH).

3D growth and clonogenic assay. A clonogenic assay was performed as described in (18). In brief, 10⁴ cells were mixed with DMEM/10% FBS containing 0.3% agarose and were layered over a solid base of 0.5% agarose in the same medium. After 15 days of incubation at 37°C, colonies were stained and counted.

Spheroid growth was achieved by seeding 2,500 cells, resuspended in 100 μ l complete cell culture medium supplemented with 0.24% MethoCell (Merck KGaA) in each well of a 96-well round-bottom low-adhesion cell culture plate (Greiner Bio-One GmbH). Seeded cells were grown under standard temperature and CO₂ conditions until the formation of spheroids (usually 5 days).

Isolation of cell clones. COUP-TFII_V2 and COUP-TFII_V1 PANC-1 cells were obtained by serial dilution of PANC-1 cells transiently transfected with COUP-TFII_V2 or COUP-TFII_V1 plasmids. Transfections were performed with FuGENE HD transfection reagent (Promega Corporation) according to manufacturer's protocol. Serial dilutions were performed 48 h after transfection; selection of transfected cells was carried out exposing the transfected cells to 3.2 mg/ml

G418 (Invitrogen; Thermo Fisher Scientific, Inc.). Similarly, MOCK PANC-1 cells were obtained after transfection with pcDNA3.1(+) plasmid and PANC-V2NLS were obtained transfecting the PANC-1 cells with the COUP-TFII_V2NLS plasmid. The expression of the COUP-TFIIs was verified by western blot analysis.

Patients. A total of 43 PDAC tissues were obtained after written informed consent from patients that underwent surgical resection at the Surgery Unit of Careggi University Hospital (Firenze, Italy) between February 2013 and December 2018. The study was approved by Careggi University Hospital Ethical Committee (Firenze, Italy; no. 0028114). Inclusion criteria were admission to surgery for PDAC; exclusion criteria were the absence of consent and the presence of comorbidities that may influence survival. The diagnosis was performed after surgery. Of the 43 PDAC samples collected, three were discarded due to the absence of amplification of the house-keeping genes and two had no detectable COUP-TFII_V2 expression (Table I). The median follow-up of the study population was 412.5 days and the median survival time was 644 days; 23 subjects were female and 17 male, with a median age of 70 years. All patients received gemcitabine as adjuvant therapy and none received any neo-adjuvant treatments.

RNA extraction and reverse transcription-quantitative (RT-q)PCR. Total RNA was extracted with TRI-Reagent (MilliporeSigma) or with RNeasy mini kit (Qiagen). Subsequently, 100 ng to 1 μ g RNA was reverse transcribed with the High-capacity RNA-to-cDNA master mix (Thermo Fisher Scientific, Inc.), whereas qPCR was performed

with GoTaq qPCR Master Mix (Promega Corporation) on an AbiPrism 7000 (Thermo Fisher Scientific, Inc.). Quantification of relative expression was performed with the $2^{-\Delta\Delta C_t}$ method with DataAssist software 3.01 (RRID:SCR_014969; Thermo Fisher Scientific, Inc.) or with LinRegPCR 2020.0 (<https://www.medischebiologie.nl/files/>). GAPDH and RPL13A were used as internal controls and their resulting geometric mean was used for normalization. The primers are listed in Table SII.

Western blot analysis, COUP-TFII_V2-specific antibody and proteomics. SDS-Page western blot was performed as previously described (18,21). Relative quantification of western blot data was performed with the Gel analysis function of ImageJ 1.52r inside Icy 2.0.3. Immunoprecipitation (IP) was performed with 'Protein A/G PLUS-Agarose Immunoprecipitation reagent' (cat. no. sc-2003; Santa Cruz Biotechnology, Inc.), according to the manufacturer's instruction. Nuclear extraction was performed with the 'Nuclear extraction kit' (cat. no. 2900; Chemicon International) according to the manufacturer's instructions. A rabbit polyclonal COUP-TFII_V2 antibody was generated by Genecust Europe using the N-terminal region of V2 as the antigen; its reactivity and specificity were tested by western blot, immunohistochemistry (IHC) and immunofluorescence (IF); the COUP-TFII_V2 antibody was used at the following dilutions: 1:50 (WB), 1:25 (IHC) and 1:100 (IF). Antibodies used for WB were as follows: COUP-TFII_V1 (cat. no. ab41859; 1:500 dilution; Abcam), COUP-TFII (cat. no. ab50487; 1:1,000 Abcam), β -catenin (cat. no. sc-7963; 1:1,000; Santa Cruz Biotechnology, Inc.); ERK (cat. no. sc-94; 1:100; Santa Cruz Biotechnology, Inc.); phosphorylated (P)-ERK (cat. no. sc-7383; 1:200; Santa Cruz Biotechnology, Inc.); AKT (cat. no. 9272; 1:1,000; Cell Signaling Technology, Inc.); P-AKT (cat. no. 9271; 1:1,000; Cell Signaling Technology, Inc.); AMPK (cat. no. 2603; 1:1,000; Cell Signaling Technology, Inc.); P-AMPK (cat. no. 4188; 1:1,000; Cell Signaling Technology, Inc.); forkhead box (FOX)O3a (cat. no. ab47409; 1:1,000; Abcam); P-FOXO3a (cat. no. ab47285; 1:1,000; Abcam); P-GSK3 (cat. no. 8566; 1:1,000; Cell Signaling Technology, Inc.); GSK3 (cat. no. 5676; 1:1,000; Cell Signaling Technology, Inc.); vimentin (cat. no. M0725; 1:1,000; DAKO); GAPDH (cat. no. G8759; 1:10,000; MilliporeSigma); BRG1 (cat. no. ab70558; 1:1,000; Abcam); Histone H3 (cat. no. Ab10799; 1:1,000, Abcam); HSP70 (cat. no. sc-24; 1:1,000; Santa Cruz Biotechnology, Inc.); FAK (cat. no. sc-558; 1:200; Santa Cruz Biotechnology, Inc.); Vinculin (cat. no. V9131; 1:1,000; MilliporeSigma); P21 (cat. no. ab7960; 1:200; Abcam); pP21 (cat. no. ab47300; 1:500; Abcam); RhoA (cat. no. sc-418; 1:100; Santa Cruz Biotechnology, Inc.); Ubiquitin (cat. no. SPA-203; 1:1,000; Stressgene Corp.); β -tubulin (cat. no. T5201; 1:500, Sigma).

Proteomics experiments and Differential in Gel Expression (DIGE) were performed as previously described (22). Specifically, total protein was extracted from subconfluent PANC-1 clones (MOCK, COUP-TFII_V1 and COUP-TFII_V2). From each clone, three protein extracts were combined. Fifty micrograms of cyanine 3 (Cy3)- or Cy5-labeled proteins were electrofocused on Dry Strip gel pH 3-10 nl immobiline strips (Cytiva) together with 50 μ g of a Cy2-labeled pool of proteins coming from the three clones. Differentially expressed proteins were then identified by mass spectrometry (22).

Gene ontology (GO) and Reactome pathway analysis were performed with the Cytoscape (RRID:SCR_003032) ClueGO plugin (RRID:SCR_005748) (23). The ontology database was updated to the version published in August 2019.

IHC, IF and collagen staining. IHC and IF with antibodies to COUP-TFII_V1 (cat. no. AB41859; RRID:AB_742211) and cytokeratin (CK)19 (cat. no. AB15463; RRID:AB_2281021; both from Abcam) were performed as previously described (18,24). The custom-made primary antibody for COUP-TFII_V2 was used at 1:25 dilution in PBS containing 2% BSA (MilliporeSigma) and 0.01% Triton X-100 (Sigma). IHC for α -smooth muscle actin was performed with the monoclonal clone A4 (DAKO; Agilent Technologies, Inc.) diluted 1:100 in PBS with 2% BSA and 0.01% Triton X-100 following the previously described protocol; the sections were incubated with an M.O.M. kit (Vector Laboratories, Inc.) prior to incubation with the primary antibody. For β -catenin IF the same antibody used in western blot was used diluted 1:50; SMAD2/3P IF was performed with a 1:100 dilution of a rabbit polyclonal antibody (cat. no. ab272332; Abcam); actin filaments were decorated with Alexa Fluor 633 phalloidin (Molecular Probes cat. no. A22284); cell nuclei were stained with DAPI (cat. no. 10236276001; Roche). Collagen was stained with standard Sirius Red staining. Sirius Red was quantified with ImageJ 1.52r under Icy 2.0.3 on images with RGB color settings; the selection of stained areas was achieved with the function 'Color threshold'.

Expression in primary tissues. COUP-TFII_V2 expression in primary PDAC tissues was determined by RT-qPCR of RNA extracted from 4-5 30 μ m-thick formalin-fixed and sucrose-protected tumor cryo-sections; the expression of COUP-TFII_V2 was confirmed by IHC on selected samples. For IHC, the custom anti-COUP-TFII_V2 rabbit polyclonal antibody was used diluted 1:25 in PBS with 2% BSA and 0.01% Triton X-100; incubation with the antibody was performed overnight (O/N) at 4°C in a humidified chamber. Prior to primary antibody incubation, sections were preblocked with 2.5% NGS for 1 h at room temperature (ImmPRESS® HRP Horse Anti-Rabbit IgG Polymer Detection Kit, Peroxidase, RRID:AB_2336529; Vectorlabs). Citrate buffer (pH 6.0) was used for antigen retrieval (100°C for 10 min) before primary antibody incubation and pre-blocking of tissue sections; an anti-rabbit HRP polymer contained in the above-mentioned kit was used as the secondary antibody; sections were incubated with the polymer for 30 min at room temperature in a humidified chamber. Semiquantitative scoring of PDAC was performed on 22 samples by two expert pathologists. Points were given according to the intensity of the staining (no staining, 0 points; low, 1 point; moderate, 2 points; and strong, 3 points); and the percentage of cells expressing the nuclear receptor (<10%, 1 point; \geq 10% and <50%, 2 points; \geq 50 and <80%, 3 points; \geq 80%, 4 points). The final score was multiplicative and PAD expression was considered low when the final score was <6. Cohen's kappa coefficient of concordance (25) between IHC semi-quantitative analysis and qPCR was calculated in R with the library 'vcd'. Results of the concordance analysis between the qPCR score and IHC score are provided in Fig. S1.

In vivo experiment. Athymic nude male mice (Fox1^{nu/nu}; age, 6 weeks; body weight, 22 g) were purchased from Harlan and kept under sterile conditions under a 12-h light/dark cycle with chow and water provided *ad libitum*. PANC-1 clones (MOCK, PANC-V1 and PANC-V2) were harvested, suspended at a concentration of 10⁶ cells/50 μ l PBS and injected into the tail of the pancreas; during the surgical procedure, the mice were anesthetized with an intraperitoneal injection of ketamine/xylazine (100 and 10 mg/kg, respectively). A total of 15 animals were used, 5 in each experimental group. After surgery, the animals were checked daily. At two weeks after the surgery, the mice were euthanized by cervical dislocation; death was verified by the absence of heartbeat and respiration. Thereafter, the pancreas and adjacent organs were collected for histology evaluation. The tumor score was based on a variation of the score reported in (26); final score was additive; the score point allocation system is provided in Table SIII. All experiments were performed following the guidance for the use of laboratory animals and were approved by the appointed authority under Italian law (Ministry of Health; Rome, Italy; no. 853/2015-PR) (27). None of the mice was found dead and no animal reached the humane endpoints of the experiment, which were weight loss >20%, no movement for >24 h, ulceration at the site of the surgical procedure with organ exposure and breathing difficulties (e.g. apnea).

Oligo annealing. Labeled nucleotide corresponding to the COUP-TFII binding site in the sodium-hydrogen exchanger (NHE) pump promoter were synthesized by MilliporeSigma and purified by HPLC (oligo sequences are provided in Table SIV). Oligos were resuspended at 1 mg/ml in molecular biology-grade water. For the annealing, 30 ng of each set of oligos per gel shift reaction were diluted in annealing buffer (100 mM Tris HCl pH 8.0, 100 mM EDTA pH 8.0, 20 mM NaCl, 5 mM MgCl₂) and denatured at 95°C for 3 min in a thermomixer (Eppendorf), then allowed to slowly cool to RT. Annealed oligos were stored at -20°C.

Gel shift. Gel shift experiments were performed according to the protocol described in (22) with a Cy3-labeled oligo-nucleotide corresponding to the COUP-TFII binding site in the NHE promoter (28). Total proteins were extracted from PANC-1 cells 48 h after transfection with a control plasmid, COUP-TFII_V1 or COUP-TFII_V2. For the binding reaction, 50 μ g of proteins were incubated for 1 h at 4°C in a binding reaction with Cy3-labeled oligos (Table SIV) (no differences in binding to labeled oligos were detected among incubation times ranging from 1 h to O/N, data not shown). For gel shift, total protein extracts were pre-incubated O/N at 4°C with 0.1 mg/ml of the same COUP-TFII_V1 mouse monoclonal antibody used for IF, western blot and IHC; the following day, the labeled oligonucleotide was added to the reaction mix for 1 h at 4°C. The product mixtures were then run on 5% non-denaturing Tris-borate EDTA (TBE, 45 mM Tris-borate buffer with 1 mM EDTA)-polyacrylamide gel and run with TBE buffer for 10 h at 4°C.

NHE reporter and Gli transcription factor activity assay. NHE reporter and Gli activity were evaluated with the Dual Luciferase Assay system (Promega Corporation). Briefly,

cells were transfected with NHE reporter plasmid or with Gli reporter, together with a minimal promoter *Renilla* reporter plasmid (Promega Corporation) (at a 1:100 ratio with respect to the target plasmids). The transfections were carried out in suspension with FuGENE HD (Promega Corporation) and 10,000 cells/well were plated in 96 wells plates. Readout was performed with a Glomax 96 microplate luminometer Dual injector system (Promega Corporation) 48 h after transfection.

Statistical analysis. Each experiment was performed in triplicates unless otherwise stated. Statistical analysis was performed with R 4.1 (www.r-project.org; RRID:SCR_001905) and Jamovi 2.0 (www.jamovi.org; RRID:SCR_016142). Differences in experimental results were evaluated by Student's t-test or the Mann-Whitney U test (Wilcoxon Rank-sum test), abbreviated as 'Wilcoxon' when reported in the figures, for parametric and non-parametric data, respectively. When comparing multiple groups, ANOVA followed by Tukey's highly-significant differences post-hoc test was used for parametric data, while the Kruskal-Wallis test followed by the Conover-Iman test was used for pairwise comparisons of non-parametric data (29). Normality of data distribution was assessed with the Shapiro-Wilk normality test. Hierarchical clustering was performed using R with the 'pheatmap' library. Survival and Cox analyses for this study cohort were performed with the 'survival', 'survminer' and 'ggforest' libraries. Cohen's concordance was calculated with the 'vcd' library in R. Values are expressed as the mean \pm standard deviation unless otherwise stated. P<0.05 was considered to indicate statistical significance. Principal component analysis (PCA) was performed with 'prcomp' under R 4.1. The graphical representations of the experimental results were generated with the 'ggpubr' and 'ggplot2' R libraries and final images were mounted with Scribus 1.5.4 (<https://www.scribus.net>) or Inkscape 1.0 (<https://www.inkscape.org>).

Results

COUP-TFII_V2 is highly expressed in PDAC and affects patient survival. As a previously published study by our group indicated that human PDAC cells express COUP-TFII_V1 (18), the present study sought to demonstrate the expression of COUP-TFII_V2 in human PDAC cells. As presented in Fig. 1A, COUP-TFII_V2 mRNA was detectable in all tested PDAC cell lines (from the well-differentiated and K-RAS wild-type BxPC3 to the poorly differentiated PANC-1). The expression was lower in PANC-1 and higher in Su.86.86 cells. Gene clustering suggested that COUP-TFII_V1 and COUP-TFII_V2 share expression patterns similar to Kruppel-like factor (KLF)4, KLF6 and NANOG (Fig. 1B), while the PCA-biplot indicated a correlation of COUP-TFII_V1 and V2 with SNAIL1; furthermore, PCA suggested that the receptors are a characterizing factor of the metastatic cell line Su.86.86 (Fig. S2A). These data suggest that both isoforms are associated with stemness and metastatic potential. Of note, COUP-TFII_V2 expression was not limited to the nucleus but spanned to the cytosol (Figs. 1C and S2B-D), whereas V1 was strictly nuclear-specific (Fig. S2E) (5,18). Furthermore, COUP-TFII_V2 localization exhibited cell-to-cell variation, having a stronger cytoplasmic expression in certain cells

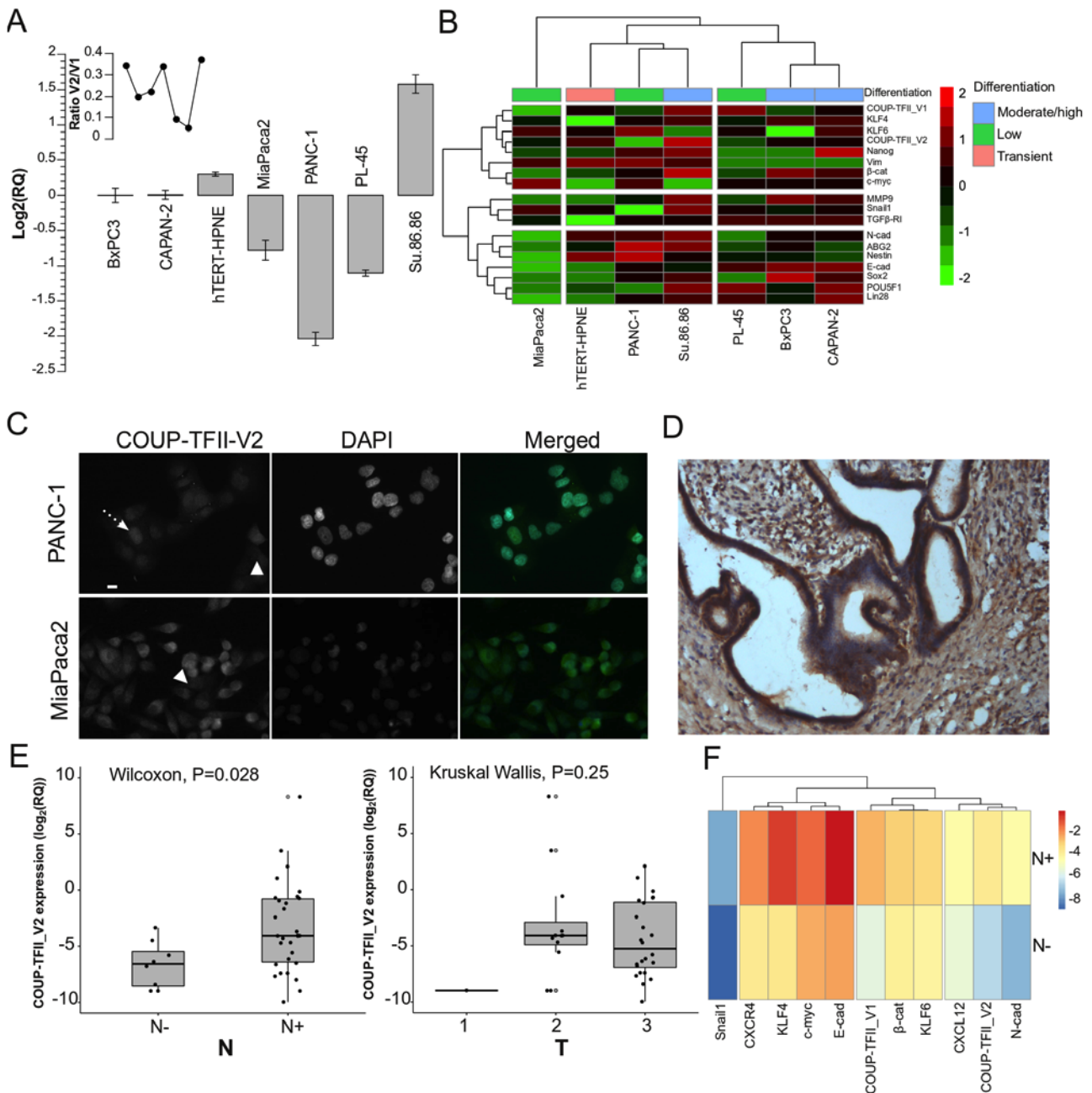


Figure 1. COUP-TFII_V2 expression. (A) Reverse transcription-quantitative PCR analysis of COUP-TFII_V2 in cancer cell lines. The results suggested that COUP-TFII_V2 mRNA expression was not associated with cell differentiation. Expression data refer to the BxPC3 cell line. (B) Complete hierarchical clustering with Euclidean distance of a panel of genes in PDAC cell lines. (C) Immunofluorescence analysis of native COUP-TFII_V2 in PANC-1 (upper panel) and MiaPaca2 (lower panel) cells performed with a custom-made polyclonal antibody (first panel in each group). The receptor is localized in the nucleus and cytosol. White arrows indicate cells with limited nuclear expression; dotted arrows indicate cells with a predominant nuclear expression (scale bar, 10 μ m). (D) Representative immunohistochemistry image of COUP-TFII_V2 in primary PDAC (magnification, x100). Sections were counterstained with Gill's hematoxylin no III. Brown staining is considered to indicate positivity. (E) COUP-TFII_V2 expression is significantly increased in the presence of lymph node metastasis with no difference for T stage. Gray-filled circles mark the position of outliers. (F) Cluster analysis of genes in N+ and N- PDAC patients. TF, transcription factor; PDAC, pancreatic ductal adenocarcinoma; N, nodal status; T, tumor stage.

(Figs. 1C and S2B). In primary tumors, COUP-TFII_V2 was expressed in the cancer cells (Figs. 1D and S3A-H) and its mRNA expression was predictive of advanced disease (Table I). Specifically, COUP-TFII_V2 expression was significantly higher in patients with lymph node metastasis (Figs. 1E and S3I), suggesting that this nuclear receptor may be associated with tumor spreading. No specific associations with age, sex or other clinicopathological characteristics were observed (Table I). When confronting the average gene

expression between N0 and N+ patients, the hierarchical clustering indicated a close association of COUP-TFII_V2 with N-cadherin and C-X-C motif chemokine ligand (CXCL)12, while COUP-TFII_V1 was linked to β -catenin and KLF4 (Fig. 1F). Considering each PDAC patient separately, V1 was associated with the expression of CXCR4 and KLF4, whereas V2 was associated with CXCL12 and N-cadherin (Fig. 2A); similar results were obtained with a correlation analysis of gene expression (Fig. S4). Kaplan-Meier survival analysis

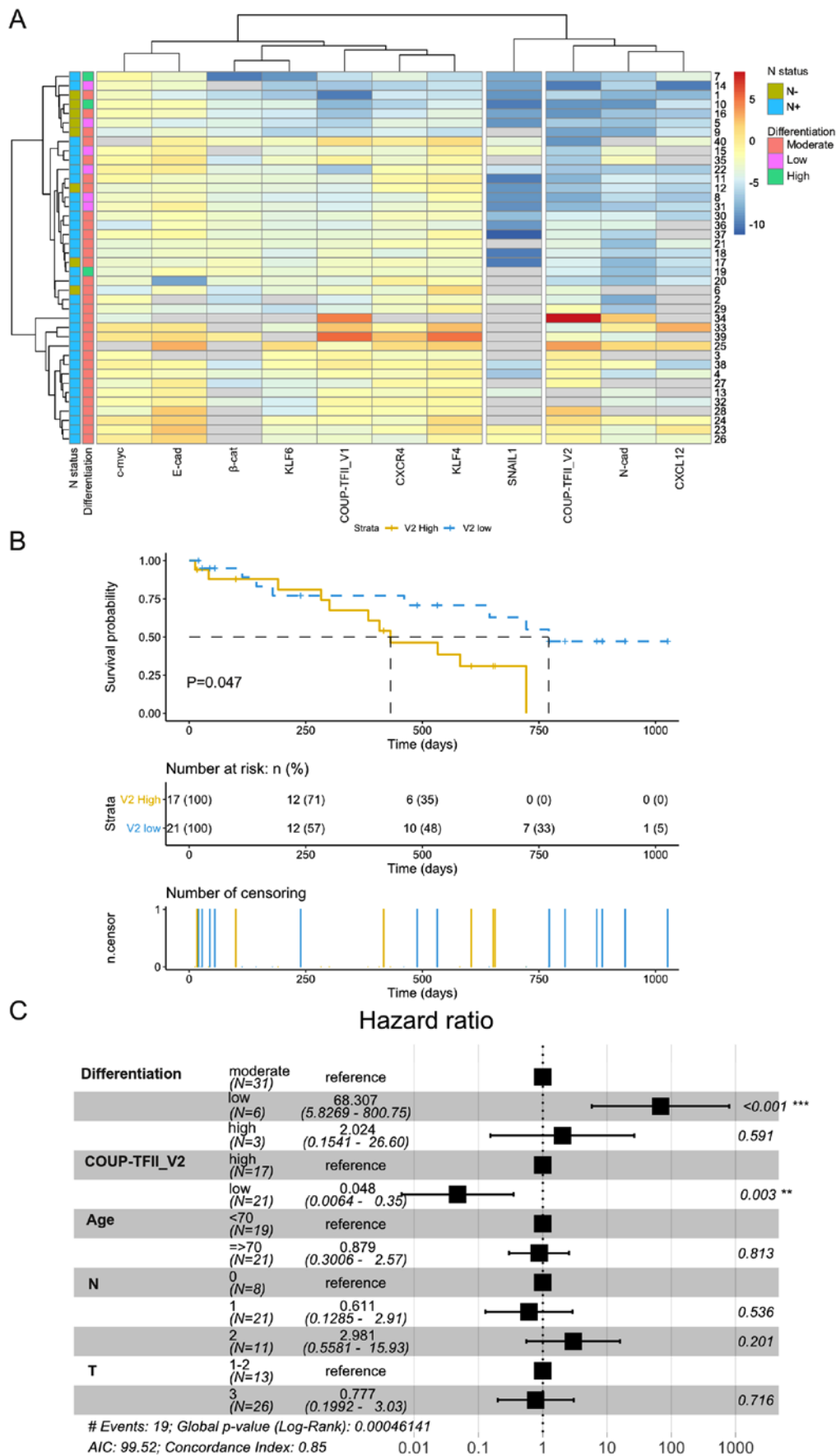


Figure 2. COUP-TFII_V2 influences the survival of PDAC patients. (A) Gene clustering in PDAC primary tumors. (B) Kaplan-Meier survival curves indicating that patients with high expression of COUP-TFII_V2 (defined as an expression of ≥ 0.06 arbitrary units, corresponding to the median COUP-TFII_V2 expression in N+ patients), had significantly lower overall survival compared to patients with low expression of COUP-TFII_V2 (P=0.043, log-rank test). (C) Cox multivariate analysis of the influence of risk factors on survival in primary PDAC. TF, transcription factor; PDAC, pancreatic ductal adenocarcinoma; N, nodal status; T, tumor stage; AIC, Akaike's Information Criterion. **P<0.01; ***P<0.001.

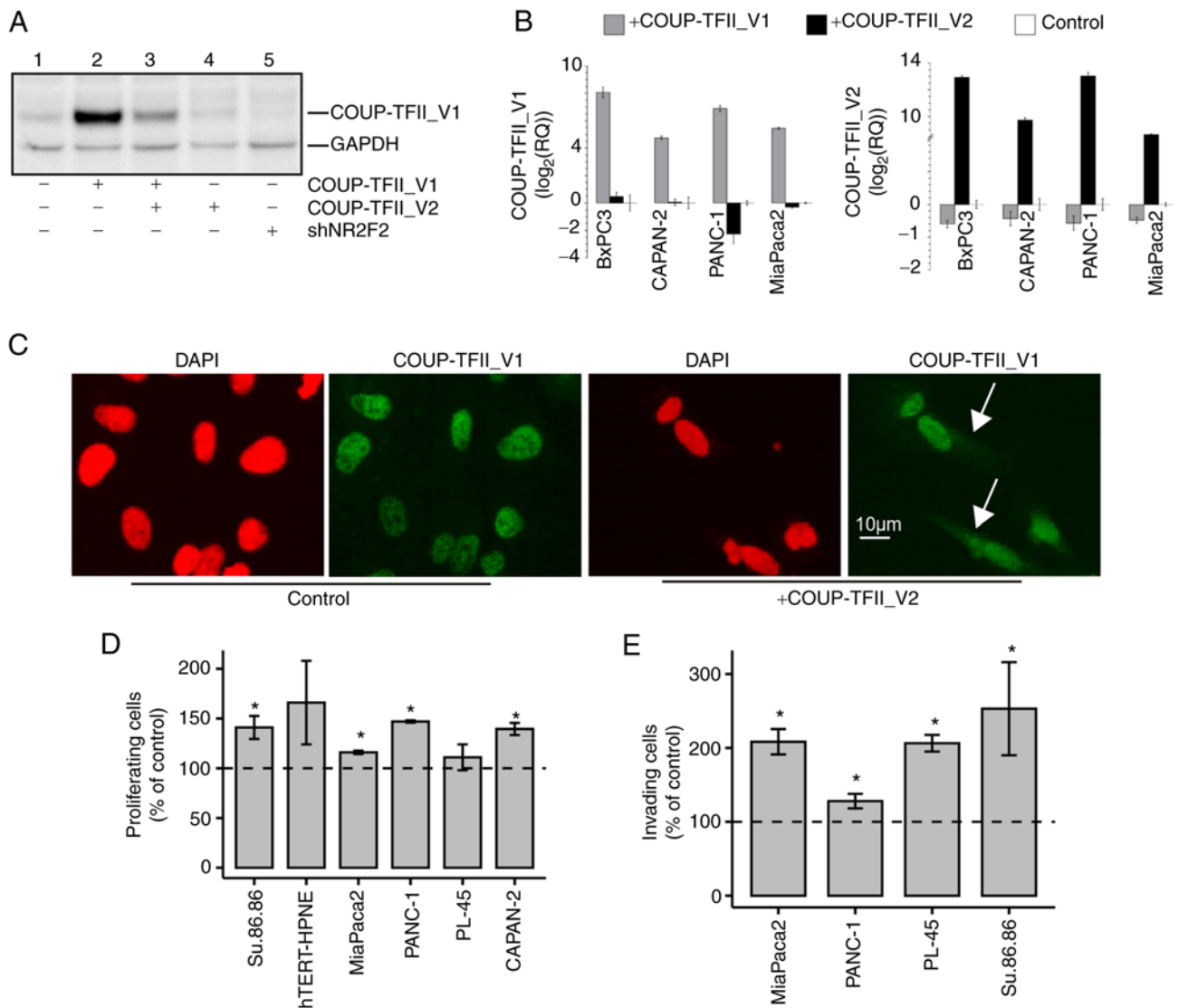


Figure 3. (A) Western blot analysis of PANC-1 cells transiently transfected with a fixed amount of COUP-TFII_V1 plasmid with and without COUP-TFII_V2 co-transfection (lanes 2-3) or COUP-TFII_V2 alone (lane 4) or a plasmid for COUP-TFII shRNA (shNR2F2, lane 5). Co-transfection of COUP-TFII_V2 reduced the expression of COUP-TFII_V1, with an effect similar to that obtained with the shRNA. Cells in lanes 1-4 were co-transfected with shNEG. (B) COUP-TFII_V1 (left panel) and COUP-TFII_V2 (right panel) expression detected by reverse transcription-quantitative PCR in pancreatic ductal adenocarcinoma cells. Cells were transfected with COUP-TFII_V1- or COUP-TFII_V2-expressing plasmids for 72 h prior to RNA extraction. (C) COUP-TFII_V1 immunofluorescence in COUP-TFII_V2-overexpressing cells. In hTERT-HPNE cells, COUP-TFII_V2 expression modified the cellular morphology and COUP-TFII_V1 compartmentalization, causing its cytosolic localization (scale bar, 10 μ m). (D) Cell viability tests were performed at 48 h (hTERT-HPNE, PANC-1, MiaPaca2, Su.86.86) or 72 h (PL-45 and CAPAN-2) after COUP-TFII_V2 transfection. Data are normalized to viable cells in pcDNA3.1-transfected cells. (E) The invasiveness of MiaPaca2, PL-45 and PANC-1 cells was increased after COUP-TFII_V2 overexpression. Data are normalized to invading cells in controls. Values are expressed as the mean \pm standard deviation. * $P < 0.05$ vs. control. shRNA, short hairpin RNA; shNR2F2, shRNA targeting NR2F2 (COUP-TFII); shNEG, negative control shRNA; NR2F2, nuclear receptor 2 family 2; TF, transcription factor.

indicated that patients with high expression of COUP-TFII_V2 had a significantly shorter overall survival (432 vs. 771 days, $P = 0.047$) (Fig. 2B) and Cox multivariate analysis demonstrated that patients with low expression of COUP-TFII_V2 or a higher degree of differentiation had a lower hazard ratio (Fig. 2C), confirming the results of the Cox univariate analysis (Table SV). The influence of clinical parameters on the survival in the study population is provided in Fig. S5.

COUP-TFII isoforms reciprocally regulate their expression and cell localization. To determine the role of COUP-TFII_V2, PDAC cell lines were transiently transfected with this receptor isoform. In MiaPaca2 and PANC-1,

overexpression of COUP-TFII_V2 reduced the mRNA and protein levels of COUP-TFII_V1, mimicking the effects of siRNA silencing (Figs. 3A and B and S6A-E). Of note, overexpression of COUP-TFII_V1 consistently decreased V2 expression (Fig. 3B), suggesting a negative feedback loop between the isoforms. In addition, Co-immunoprecipitation demonstrated that the variants are associated (Fig. S6F). Indeed, COUP-TFII_V2 overexpression delocalized COUP-TFII_V1 in the cytosol as demonstrated by IF in hTERT-HPNE (Fig. 3C). This result was confirmed by co-transfection experiments in PANC-1 cells with the EGFP-COUP-TFII_V1 and V2 isoforms (Fig. S6G). Furthermore, the interaction of COUP-TFII_V2 with COUP-TFII_V1 reduced the ability of

the latter to bind the DNA, as demonstrated by Gel shift and NHE reporter activity (Fig. S7).

COUP-TFII-V2 confers drug resistance and increases anchorage-independent growth and cell motility. COUP-TFII_V2 overexpression had a modest effect on proliferation in PANC-1, MiaPaca2, CAPAN-2 and Su.86.86 cells; however, transient COUP-TFII_V2 overexpression increased cell invasion in all tested lines (Fig. 3D and E). Consequently, the present study further focused on PANC-1 cells that express less of the COUP-TFII_V2 isoform and PANC-1 clones overexpressing COUP-TFII_V1 (PANC-V1) or COUP-TFII_V2 (PANC-V2) isoforms or simply resistant to G418 (MOCK) were generated. In these models, COUP-TFII-V2 overexpression significantly limited the effect of chemotherapy (Fig. 4A and B). The IC₅₀ of gemcitabine for PANC-V2 was higher than that for the control and V1-expressing cells (IC₅₀: 1, 0.130 and 0.036 μ M for PANC-V2, MOCK and PANC-V1, respectively). The higher sensitivity of V1-expressing cells to gemcitabine was indirectly confirmed by western blot analysis, as a greater reduction of COUP-TFII_V1 compared to COUP-TFII_V2 protein levels was observed after gemcitabine treatment in cells overexpressing COUP-TFII_V1 or V2 isoforms, respectively (Fig. S8A). In addition, PANC-V2 exhibited higher proliferation than MOCK or PANC-V1 cells and they formed more colonies in soft agar, suggesting increased anchorage-independent growth and tumorigenicity (Fig. 4C and D). The increased chemoresistance and proliferation of V2-expressing cells was maintained during the 3D growth (Figs. 4E and S8B and C). Time-lapse experiments with PANC-1 transfected with EGFP-COUP-TFII proteins indicated that only COUP-TFII_V2 significantly increased cellular motility (0.37 ± 0.02 vs. 0.26 ± 0.017 μ m/sec, COUP-TFII_V2 vs. control, $P<0.01$) (Fig. 4F). Similar results were obtained when tracking GFP-positive cells (1/10 of total transfection) in co-transfection experiments with untagged COUP-TFII_V1, COUP-TFII_V2 or empty plasmid (data not shown). These results were further confirmed by the wound-healing assay (Figs. 4G and S8D).

Increased COUP-TFII_V2 expression facilitates tumor growth and spreading in vivo. To evaluate the different contributions of the two COUP-TFII isoforms in tumor progression, MOCK, PANC-V1 and PANC-V2 cells were implanted in the pancreas of nude mice (Fig. 5A-D). After 2 weeks, the tumor engraftment ratio was 4/5, 3/5 and 5/5 for MOCK, PANC-V1 and PANC-V2 mice, respectively. Of note, 4 out of 5 PANC-V2 xenografts exhibited liver metastasis compared to just 1 in the PANC-MOCK and none in the PANC-V1 group; local diffusion to the adjacent tissues, such as the spleen, was instead present in almost all engrafted animals and the maximum tumor size observed was 18 mm (data not shown). Accordingly, the tumor score and tumor weight were significantly higher for PANC-V2 tumors ($P<0.05$ vs. PANC-V1 and MOCK tumor-bearing mice) (Fig. 5B). Immunostaining for PCNA and activated Caspase 3/7 of the tumors indicated that proliferation and apoptosis were significantly altered in PANC-V2-bearing mice (Fig. 5C and D). No clear differences in stromal reaction (as demonstrated by Sirius Red Collagen staining and quantification) and stromal infiltration were detected (Fig. S9).

COUP-TFII_V2 influences stemness and senescence. In consideration of the role of COUP-TFII in the stemness and cell fate determination (29), it was assessed whether COUP-TFII_V2 affects cell stemness. COUP-TFII_V2 specifically increased the expression of NANOG, Nestin, c-Myc and human telomerase reverse transcriptase, genes that are downregulated or not altered in V1 (Fig. 5E). On the other hand, COUP-TFII_V1 is associated with increased SOX2 and KLF4 and decreased expression of KLF6, which are associated with a higher tumor potential in PDAC (30-33). Similar results were obtained in transiently transfected BxPC3, MiaPaca2, CAPAN-2 and PANC-1 cells and in cells growing in 3D (Fig. S10A and B). These differences were associated with significantly increased senescence and cell size of COUP-TFII_V1-expressing cells (Figs. 5F and G and S10C).

Proteome of COUP-TFII-expressing cells. To better characterize the function of COUP-TFII isoforms, an exploratory proteomic analysis was performed on PANC-V2 and PANC-V1 against the MOCK background. According to DIGE proteomics, 175 protein spots were altered in PANC-V1 and 147 in PANC-V2, compared to the MOCK cells. GO analysis (Figs. 6A and S11, Tables SVI and SVII) suggested that for COUP-TFII_V2, the GO terms are linked to regulation of cell metabolism, cytoskeleton and cell cycle/apoptosis. On the contrary, COUP-TFII_V1-specific GO terms point to small GTPase, response to stress and stimuli [e.g., TNF, interleukins (ILs), Hedgehog (HH) and Heatshock protein (HSP)], secretion of angiogenic factors (such as VEGF), cell-to-cell interactions and IL signaling (Tables SVIII and SIX). Reactome analysis confirmed the GO ontologies suggesting that COUP-TFII_V2 is associated with glycolysis, apoptotic cleavage of cellular proteins and cytoskeleton, whereas COUP-TFII_V1 is associated with response to stress, formation of cell-to-cell junction, Rho activity and HH signaling (Tables SVII and SIX).

COUP-TFII_V2 regulates EMT. Proteomic data, alongside the present *in vitro* results, suggested that COUP-TFII_V2 may be implicated in the regulation of EMT. In agreement with this, western blot analysis indicated increased vimentin expression in PANC-V2 cells (Fig. 6B). Furthermore, IF suggested that COUP-TFII_V2 expression, compared to COUP-TFII_V1, resulted in well-organized actin intermediate filaments and decreased expression of the epithelial marker E-cadherin. Conversely, the mesenchymal markers N-cadherin and vimentin were decreased in PANC-V1 (Fig. 6C). However, TGF β and TGF β -receptor I, considered to be associated with EMT, were not altered in cells overexpressing either of the two isoforms (Fig. 6D). Unexpectedly, PANC-V1 cells strongly responded to TGF β and had higher levels of SMAD2/3P, as suggested by IF (Figs. 6E and S12A and B). Conversely, MOCK and PANC-V2 exhibited only a modest increase in vimentin and a slight alteration of cell shape after TGF β treatment (Figs. 6E and S12A). Of note, VEGF-C, MMP9 and the cell-homing receptor CXCR4 were differentially expressed between PANC-V1 and PANC-V2 (Fig. 6D). In accordance with the alteration of the cytoskeleton and EMT, a reduction of β -catenin in PANC-V2 was observed (Fig. 6B); furthermore, the IF experiments pointed to a higher nuclear localization of β -catenin in PANC-V1 cells (Fig. S12C). The reduced protein

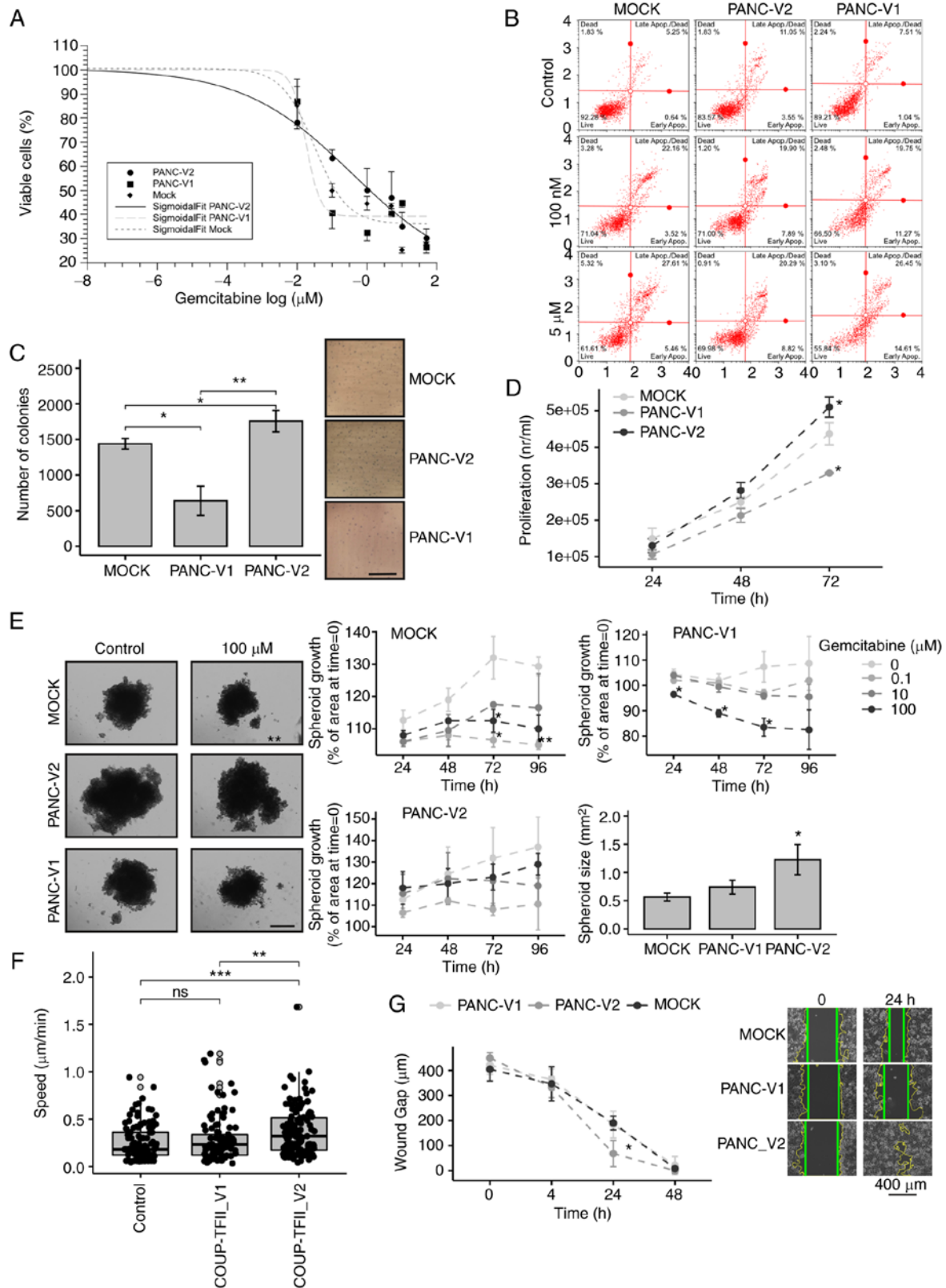


Figure 4. Biological effects of COUP-TFII_V2 expression. (A) MOCK, PANC-V1 and PANC-V2 cells were treated for 48 h with increasing concentrations of gemcitabine. Data are reported on a log scale and the dose-response curves were fitted with a Sigmoidal Boltzmann equation. (B) Annexin staining performed on PANC-1 clones treated for 24 h with gemcitabine indicated a significant increase in apoptosis of PANC-V1 and MOCK cells. (C) Colony-formation assay of PANC-1 clones (scale bar, 5 mm). (D) Conversely to PANC-V1, PANC-V2 cells had a slightly increased proliferation that became significant at 72 h after plating. (E) PANC-V2 spheroids were bigger and more gemcitabine-resistant than their MOCK counterparts (scale bar, 500 μm). (F) Cell motility (cell velocity, expressed as $\mu\text{m}/\text{sec}$) of cells transfected with enhanced green fluorescence protein-COUP-TFII_V1 or -COUP-TFII_V2 plasmids; increased motility of COUP-TFII_V2 cells compared to GFP (control) and COUP-TFII_V1 transfected cells was apparent. Gray-filled circles mark the position of outliers. (G) Wound-healing assay of PANC-1 clones. Photomicrographs are representative images at 0 and 24 h. Intermediate images are provided in Fig. S8. Wound margins were outlined in yellow, whereas the straight green lines mark the wound edges used for the distance measurement (scale bar, 400 μm). Values are expressed as the mean \pm standard deviation. * $P < 0.05$; ** $P < 0.01$; *** $P < 0.001$. ns, no significance; PANC-V1, PANC-1 cell line overexpressing COUP-TFII_V1; PANC-V2, PANC-1 cell line overexpressing COUP-TFII_V2; MOCK, PANC-1 cell line resistant to G418; TF, transcription factor.

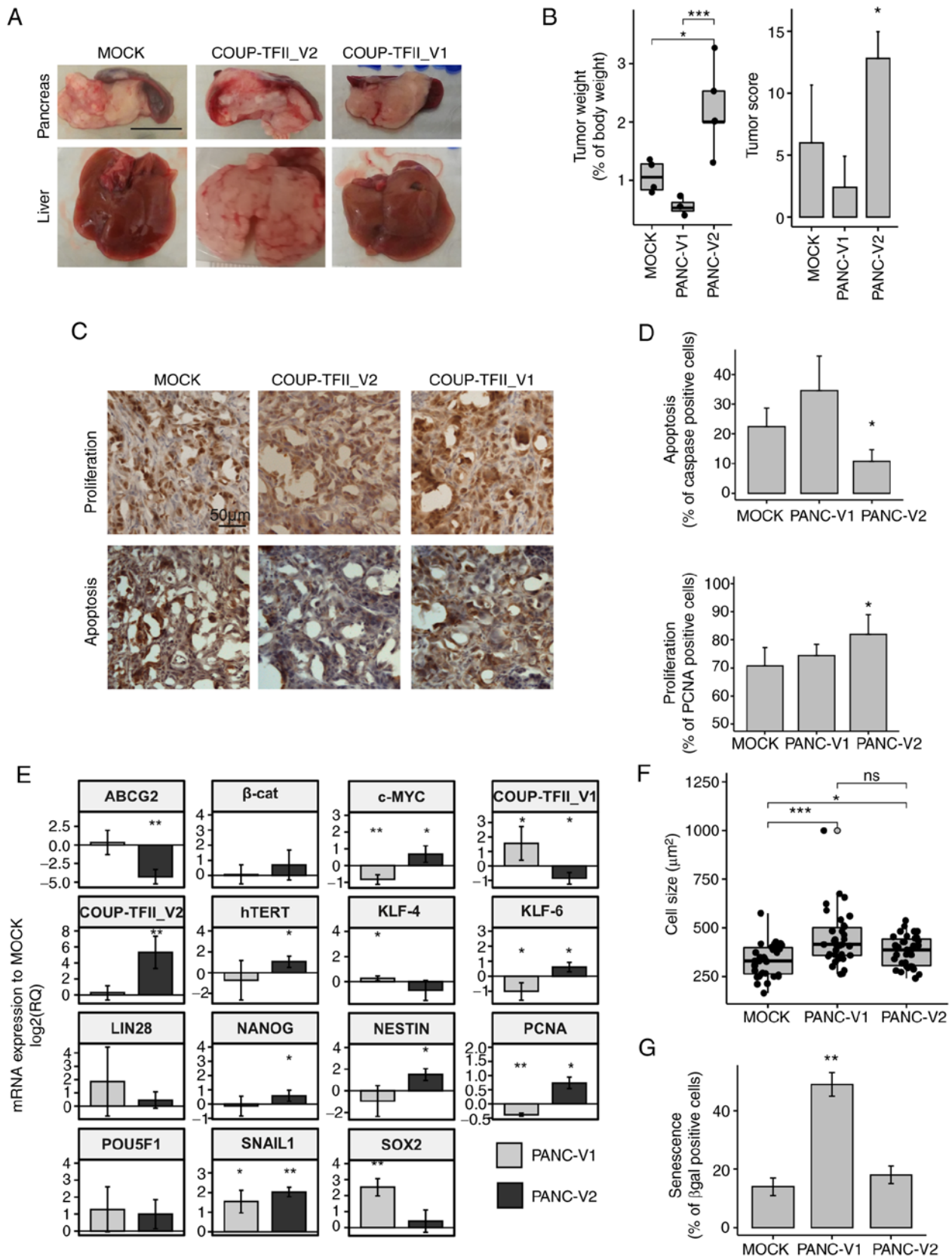


Figure 5. Regulation of gene expression and *in vivo* experiments. (A) Representative photomicrographs of livers and xenograft tumors demonstrating the metastasizing potential of PANC-V2 cells in the liver (scale bar, 1 cm). (B) Tumor weight and tumor score. (C) Representative immunohistochemistry images for PCNA and activated caspase 3/7 (scale bar, 50 μ m). (D) Quantitative analysis of proliferation and apoptosis. (E) Reverse transcription-quantitative PCR analysis of genes involved in stemness. Values are expressed as the mean \pm standard deviation of at least 3 biological replicates. (F) Cell size of PANC-V1, PANC-V2 and MOCK cells. Outliers are indicated by light gray dots. (G) Cellular senescence determined as the percentage of β -gal positive cells. Values are expressed as mean \pm standard deviation. ns, no significance; * P <0.05; ** P <0.01; *** P <0.001 (vs. MOCK when not indicated). PANC-V1, PANC-1 cell line overexpressing COUP-TFII_V1; PANC-V2, PANC-1 cell line overexpressing COUP-TFII_V2; MOCK, PANC-1 cell line resistant to G418; TF, transcription factor; β -cat, β -catenin; PCNA, proliferating cell nuclear antigen; KLF4, Kruppel-like factor 4; hTERT, human telomerase reverse transcriptase; ABCG2, ATP binding cassette Subfamily G member 2.

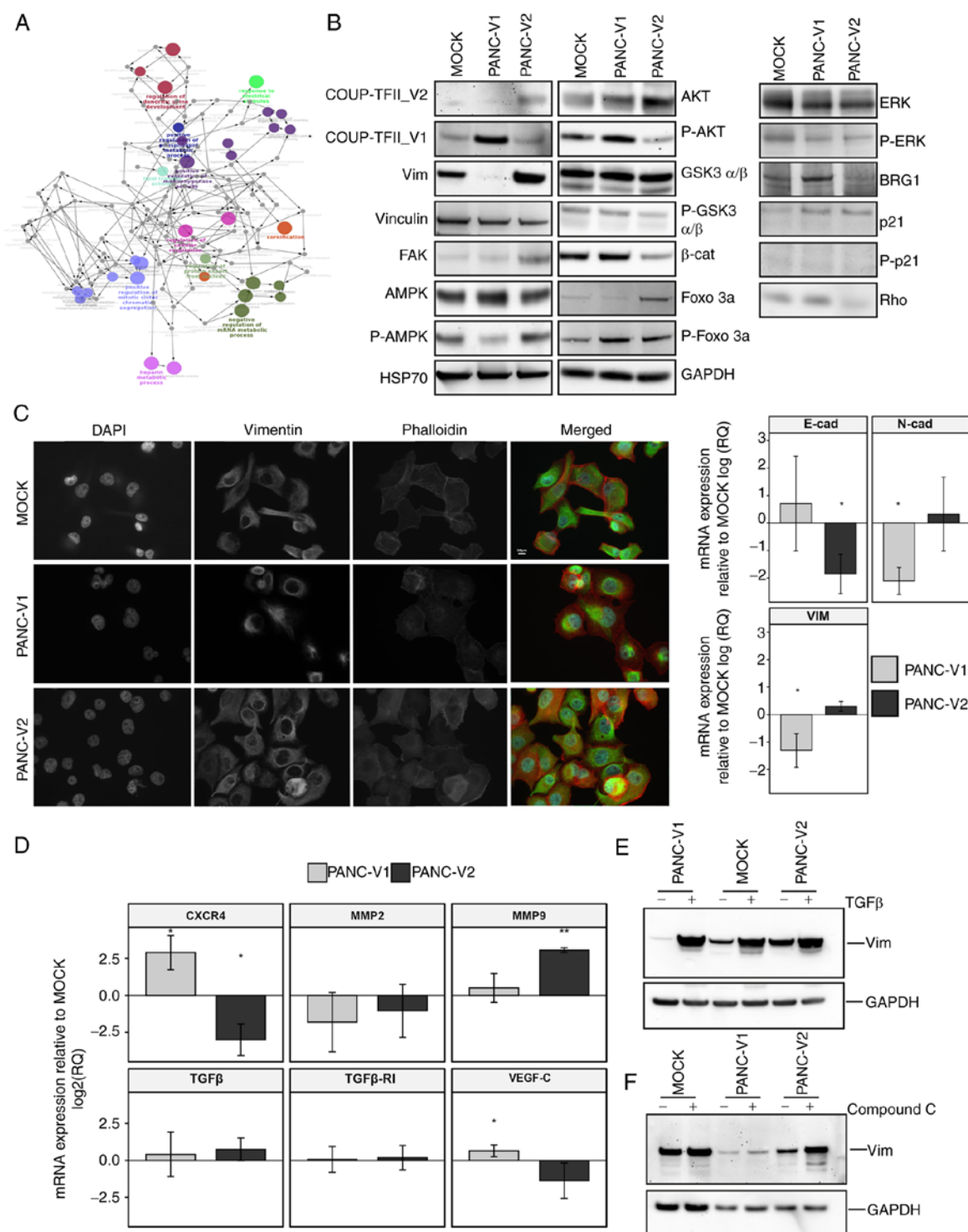


Figure 6. Signaling, gene expression and response to stimuli. (A) Network of Gene Ontology terms from ClueGO analysis of PANC-V2 cells compared to MOCK. A magnified version of this panel is reported as Fig. S15. (B) Representative western blot of PANC-V1, PANC-V2 and MOCK confluent cells. (C) Immunofluorescence analysis of vimentin and actin intermediate filaments and RT-qPCR for EMT markers N-cadherin, E-cadherin and vimentin. RT-qPCR data were normalized to the MOCK group. Scale bar, 10 μ m. (D) RT-qPCR analysis of genes linked to cell homing and modification of the micro-environment. (E) Induction of EMT mediated by TGF β in PANC-V1, PANC-V2 and MOCK groups. (F) Representative western blot of vimentin regulation after treatment with the AMPK inhibitor Compound C. Values are expressed as the mean \pm standard deviation. * P <0.05; ** P <0.01 (vs. MOCK). PANC-V1, PANC-1 cell line overexpressing COUP-TFII_V1; PANC-V2, PANC-1 cell line overexpressing COUP-TFII_V2; MOCK, PANC-1 cell line resistant to G418; TF, transcription factor; RT-qPCR, reverse transcription-quantitative PCR; EMT, epithelial to mesenchymal transition; E-cad, E-cadherin; vim, vimentin; β -cat, β -catenin; FOXO 3a forkhead box O3a; GSK3, glycogen synthase kinase 3; FAK, focal adhesion kinase.

levels of β -catenin in PANC-V2 may be explained by the decreased phosphorylation of AKT and the ensuing reduction of the inhibitory phosphorylation of its downstream target

glycogen synthase kinase (GSK)3 β ; In addition, FOXO3a phosphorylation was also increased in PANC-V1, confirming the higher AKT activity in these cells (Figs. 6B and S13A).

Similar results were obtained following transient transfection of the MiaPaca2, PL-45 and CAPAN-2 cell lines (Fig. S13B).

COUP-TFII isoforms differentially influence cell metabolism via AMPK pathway. In accordance with the isoform-dependent effect on cell metabolism emerged from the proteomic analysis, a reduction of AMPK phosphorylation was observed in COUP-TFII_V1-expressing cells. Using the mitochondrial potential as a surrogate of the cells' energetic condition, as reported in Fig. S13C, it was observed that PANC-V2 mitochondria were more depolarized compared to PANC-V1, a result that agrees with AMPK expression. Different PANC-1 clones treated with the AMPK inhibitor compound C exhibited an isoform-dependent increase of vimentin expression and induction of a mesenchymal-like phenotype (Figs. 6F and S12A), suggesting that AMPK-mediated EMT depends on the expression of COUP-TFII isoforms. In agreement with AMPK expression, Rho A, which is negatively regulated by AMPK, is decreased by COUP-TFII_V2 and increased by COUP-TFII_V1 (Fig. 6B). Of note, expression of RhoA is associated with cytoskeleton remodeling and inhibition of AMPK (34,35). Furthermore, proteomic data point to a modification of HH signaling after the expression of COUP-TFII receptors. It was previously indicated that HH may stimulate Rho A GTPase and Gli transcription factor activity is downregulated by AMPK (36,37). Confirming these data, Gli activity was increased in PANC-V1 cells (Fig. S13D); in addition, LiCl (an inhibitor of GSK3 β and HH) increased apoptosis in PANC-V1 but not PANC-V2 cells, suggesting that V2-expressing cells do not depend on HH for survival (Fig. S13E).

The function of V2 is linked to its cellular localization. COUP-TFII_V2 localization was observed to be associated with a modification of cell shape and acquisition of EMT characteristics (Fig. 7). After COUP-TFII_V2-EGFP transfection, MiaPaca2 and PANC-1 EGFP-positive cells exhibited differences in cell shape linked to the level of nuclear/cytoplasmic expression of COUP-TFII_V2 (Figs. 7A and B and S14). Accordingly, cells with mostly cytosolic COUP-TFII_V2 exhibited a pronounced mesenchymal-like phenotype (e.g., well-organized cytoskeleton or cell protrusion), while this was reduced in cells with nuclear COUP-TFII_V2, suggesting that its nuclear exclusion may potentiate EMT. To validate the hypothesis that nuclear COUP-TFII_V2 limits EMT, COUP-TFII_V2 was modified by adding an NLS to obtain the COUP-TFII_V2NLS. As indicated in Figs. 7C-F and S14, COUP-TFII_V2NLS reduced cell proliferation, cell invasion, motility and drug resistance, compared to wild-type COUP-TFII_V2-transfected cells. Of note, unlike COUP-TFII_V2, COUP-TFII_V2NLS failed to reduce the expression of COUP-TFII_V1.

Discussion

PDAC is associated with the accumulation of mutations, epigenetic modifications and alterations of cellular pathways. Although K-RAS is the most frequently altered gene, several studies have indicated that nuclear receptors are widely implicated in cancer development. Nuclear receptors may regulate processes ranging from metastatization to the modulation of the tumor microenvironment (38) with significant effects on tumor progression. COUP-TFII is a nuclear receptor that

may act as tumor suppressor or oncogene, depending on the cellular context (15,16). A previous study by our group demonstrated that COUP-TFII, in the context of PDAC, acts as an oncogene (18). In the last decade, a DBD-lacking isoform of COUP-TFII was described, but its mechanisms of action have remained elusive and were not previously evaluated in cancer (10,20). The present study indicated that both COUP-TFII isoforms are predictive of PDAC development but the results point to different actions of the receptors, suggesting a complex regulation. The present results indicated that COUP-TFII_V2 was expressed in primary pancreatic cancers and in cell lines and comparatively high expression was associated with an increased risk of death and development of metastasis. In addition, COUP-TFII_V2 expression was associated with increased tumor growth and spreading in nude mice. According to the association between COUP-TFII_V2 and advanced tumor stages, the hierarchical clustering in cell lines and patients links the receptor to EMT. Acquisition of a mesenchymal-like phenotype has a central role in the dissemination process of cancer cells and EMT-regulated mechanisms function as prognostic predictors in patients with PDAC (39). COUP-TFII_V2-induced EMT is probably mediated by the AKT and GSK3 axis, which may be consequential to PPAR γ transcriptional control (40), and it is associated with alterations of β -catenin, E-cadherin-to-N-cadherin switch and with the modulation of HH pathways. Of note, it appears that, to exert its effect on cadherin expression, V2 requires the presence of mutated K-RAS, as suggested by the opposite regulation of cadherins in K-RAS wild-type BxPC3 cells compared to CAPAN-2 cells, that are K-RAS mutated. Phosphorylation by AKT has inhibitory effects on FOXO3a and GSK3 β (41,42), and accordingly, the reduced phosphorylation of FOXO3a in V2 cells may explain the increased proliferation and the increase in the mRNA of the FOXO3a-downstream target c-myc. GSK3 belongs to the APC complex that degrades β -catenin (43) and when GSK3 β is phosphorylated, the proteasome degradation of β -catenin is reduced (44). Accordingly, β -catenin is decreased in V2-expressing cells, whereas in PANC-V1 cells that exhibit higher phosphorylation of AKT, β -catenin expression is increased. AMPK is a major sensor of the cellular metabolic condition and it may reverse or induce EMT (45). In PANC-V1 cells that exhibit signs of decreased EMT compared to MOCK and PANC-V2 cells, P-AMPK^{Tyr172} was decreased; however, inhibition of AMPK induced an increase in vimentin and it changed the cells' morphology. These results suggest a putative inhibitory role of AMPK on EMT, a hypothesis that is also supported by the higher expression of Rho A in PANC-V1 cells. Increased expression of Rho A is associated with relaxation of the contractile fibers and with the switch of cell motility from a mesenchymal to an ameboid-like movement (34,35). In this context, it may be speculated that cancer cells may switch the movement behavior quite rapidly in response to extracellular stimuli regulating the COUP-TFII_V2 or V1 expression or their cellular location. Furthermore, the reduced phosphorylation of AMPK, coupled with Rho A expression and higher mitochondrial polarization, suggest that V1-expressing cells may produce ATP more efficiently than V2. Of note, the higher V2 mitochondrial stress may lead to a higher apoptosis rate but it may also be associated with the production of reactive oxygen species that favors the K-RAS-mediated

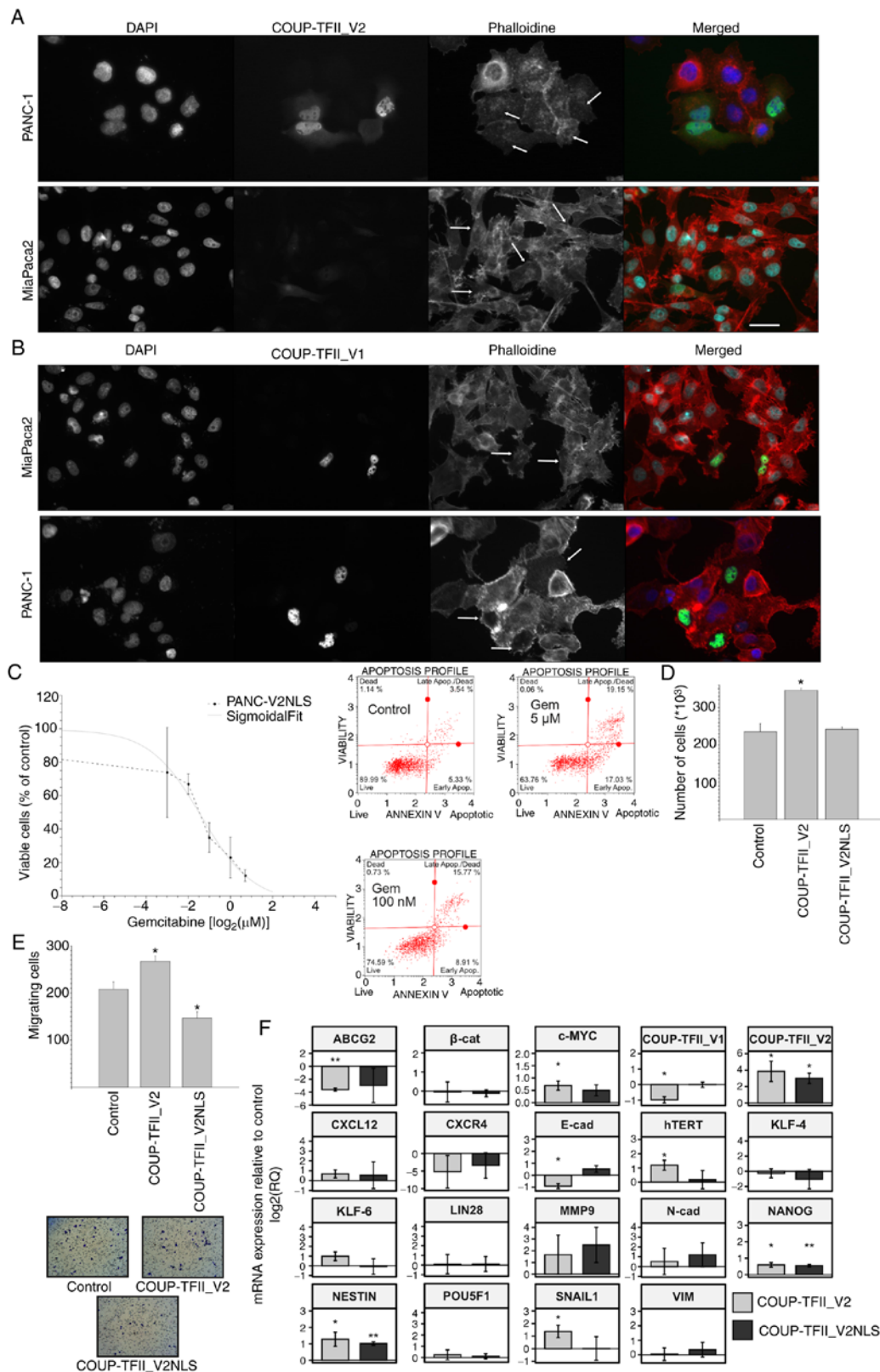


Figure 7. Nuclear localization of COUP-TFII_V2. (A and B) Immunofluorescence images for β -actin in PANC-1 and MiaPaca2 cells transfected with (A) COUP-TFII_V2-EGFP or (B) COUP-TFII_V1-EGFP. Arrows point to cells with either more nuclear or more cytoplasmic COUP-TFII_V2 and of different phenotypes, more visible in MiaPaca2 cells. Cells expressing COUP-TFII_V1-EGFP are usually flat (scale bar, 10 μm). (C) Response of PANC-V2NLS to gemcitabine indicates an IC₅₀ similar to that of MOCK cells (upper panel). The lower panel is a representative annexin plot of PANC-V2NLS cells treated with gemcitabine as presented in Fig. 4B. (D) COUP-TFII_V2NLS had no significant effect on cell proliferation. (E) Chemo-invasion of PANC-1 cells transfected with COUP-TFII_V2 or COUP-TFII_V2NLS, indicating that nuclear V2 reduces the chemoinvasiveness of PDAC cells (original magnification, $\times 100$). (F) Reverse transcription-quantitative PCR was used to assess gene expression in PANC-1 transfected with COUP-TFII_V2 or COUP-TFII_V2NLS for 48 h. Values are expressed as mean \pm standard deviation. * $P < 0.05$; ** $P < 0.01$ (vs. Control). MOCK, PANC-1 cell line resistant to G418; TF, transcription factor; PANC-V2NLS, PANC-1 cell line overexpressing a COUP-TFII_V2 with an exogenous nuclear localization signal; EGFP, enhanced green fluorescence protein. VIM, vimentin; N-cad, N-cadherin; β -cat, β -catenin; hTERT, human telomerase reverse transcriptase; ABCG2, ATP binding cassette subfamily G member 2; COUP-TFII_V2NLS, COUP-TFII_V2 with added nuclear localization sequence.

tumorigenesis (46). Taken together, mitochondrial polarization, AMPK and HH activation, which is linked to metabolic rewiring (47), may suggest that the nuclear receptor may be linked with the Warburg effect, but further experiments will be required to confirm this hypothesis. Given that PANC-V1 cells proliferate at a slower pace but do not exhibit any reduction of tumor growth *in vivo*, it may be assumed that COUP-TFII_V1 is responsible for local growth and regulates the tumor micro-environment, whereas COUP-TFII_V2 facilitates tumor spreading. Indeed, expression of COUP-TFII_V1 is associated with increased senescence paralleled by increased secretion of VEGF-C and alteration of IL and chemokine expressions, in line with a secretive-senescence phenotype that facilitates local tumor progression (48). The idea of different roles of the isoforms is strengthened by the existence of a regulatory feedback expression and by the COUP-TFII_V2-mediated regulation of the COUP-TFII_V1 transcriptional activity. Of note, COUP-TFII_V2 also influences COUP-TFII_V1 nuclear-specific localization. Of note, COUP-TFII_V2, which is clearly nuclear and cytosolic, exhibits a distinctive pattern of expression not previously described for any NR2F. How COUP-TFII_V2 shuttles between the two cell compartments is currently elusive, but its localization has clear effects on the cell phenotype. Confining the receptor to the nucleus reduces its ability to induce EMT and influences its activity on cell signaling. Indeed, the exclusive nuclear localization of COUP-TFII_V2 alters both COUP-TFII_V1 transcription and the consequent expression of stemness genes. It is conceivable that pancreatic tumor cells may respond to different microenvironmental conditions regulating COUP-TFII isoform expression in order to facilitate tumor progression. In this context, it may be speculated that the cells during the initial cancer growth may primarily express COUP-TFII_V1 to create a permissive microenvironment promoting cell-cell interaction, neo-angiogenesis (5) and regulation of immune response, then switching to a higher expression of COUP-TFII_V2, essentially for EMT and tumor spreading. Accordingly, the increase of MMP-9 mRNA after COUP-TFII_V2 overexpression may explain the higher invasiveness of tumor cells. Indeed, this gelatinase, alongside MMP-2, is a major factor in extracellular matrix degradation and it has been linked to the progression of PDAC and several other tumor types. In PDAC, MMP-9 is abnormally overexpressed but its association with survival is limited. Furthermore, in experimental models, promising results have been obtained with MMP-2 and MMP-9 inhibitors (49,50), indicating that these gelatinases are involved in PDAC progression. However, in the model of the present study, no alteration of collagen deposition was observed, as may have been expected from an increase in MMP-9; this discrepancy indicates that MMP-9 alone is not sufficient to explain the increased invasiveness of COUP-TFII_V2-overexpressing cells, given that systemic downregulation of MMP-9 may trigger metastasis in PDAC (51). Of note, nuclear receptor activities are not always mutually exclusive, and a certain degree of overlapped functions is demonstrated by similar effects on specific genes. Although a direct binding of COUP-TFII_V2 to DNA may be clearly excluded, a plausible explanation of similar effects is that COUP-TFII_V2 may act as bait for repressors in the context of specific genes, hence increasing the activity of COUP-TFII_V1 or facilitate the

action of completely different transcription factors that remain unidentified (17,29). Of note, the first exon of COUP-TFII_V2 is located upstream of the known COUP-TFII_V1 promoter (9) and another putative functional promoter exists upstream of the first exon of COUP-TFII_V2. This gene organization suggests that COUP-TFII_V2 may not be an isoform of COUP-TFII but a completely new gene.

The present study has certain limitations. First of all, the patients were recruited only in one centre, which limited the population size, and they all underwent adjuvant therapy with gemcitabine; consequently, no information was provided on the effect of COUP-TFII_V2 on survival in the presence of new chemotherapeutic regimens, such as Folfirinox. Furthermore, the *in vitro* results were obtained almost exclusively under over-expression conditions, whereas modulation by drugs, currently unavailable, may have been more similar to the physiological conditions; besides, it may have provided more useful information for future clinical applications. Furthermore, although various results of the present study were validated in numerous cell lines, AsPC1, which is one of the most aggressive pancreatic cancer cell lines, was not used; in the future, it may be worthwhile to use this cell line both *in vitro* and *in vivo* as a PDAC cancer model to enhance the knowledge on the function of COUP-TFII_V2. Finally, the regulatory factors causing the expression of either COUP-TFII_V1 or COUP-TFII_V2 were not identified, which may be pursued in the future.

In conclusion, the present study was the first to describe the effect of a novel DBD-lacking variant of COUP-TFII that was able to directly (by mediating the transcriptional activity) or indirectly (independently from transcriptional activity) act on pancreatic cancer cells' plasticity. The present results point to an efficient interaction between the COUP-TFII isoforms that confers an advantage in terms of PDAC progression and dissemination. The recent demonstration that COUP-TFII is modulated by small molecules (52) suggests that this nuclear receptor system is druggable and potentially a new therapeutic target for PDAC.

Acknowledgements

The authors thank Professor M. Vasseur-Cognet [INSERM, U1016; Department of Endocrinology, Metabolism and Cancer, Cochin Institute, CNRS (UMR 8104), Paris, France] for the kind gift of the COUP-TFII_V1 plasmid and Dr H. Sasaki (Laboratory of Embryonic Induction, RIKEN Center for Development Biology, Kobe, Japan) for the Gli reporter plasmid.

Funding

This work was supported by Fondo per gli Investimenti della Ricerca di Base (grant no. RBAP I0MY35_002), by Fondazione CR di Firenze (grant no. 2013.0673) and by FIORGEN ONLUS to AG. AG is an Investigator Grant recipient of the 'AIRC Foundation for Cancer Research' (grant no. IG 2017-20590).

Availability of data and materials

Proteomic data are deposited in PRIDE (<https://www.ebi.ac.uk/pride/>; no. PXD 030264). Other data are available from the corresponding author upon reasonable request.

Authors' contributions

SiP created the cell models, performed most of the *in vitro* experiments and WB and wrote the manuscript. SaP created the V2NLS construct, supported in experiments with V2NLS and performed the *in vivo* experiments together with MT. ST contributed by performing part of the main and preliminary experiments. EC and GM performed the proteomics analysis. IS performed part of the *in vitro* experiments and reviewed the manuscript. EG and LA provided the statistical analysis for primary samples. LB enrolled the patients and collected the primary samples. TM processed the primary samples, performed the RT-qPCR analysis and reviewed the manuscript. GD and CG processed the primary samples and performed the RT-qPCR analysis. LP performed part of the RT-qPCR analysis of *in vitro* experiments. SM contributed to analyzing the data, critically reviewed the results and corrected the main manuscript. AG defined the general goal of the research, supervised the project, enrolled the patients, reviewed the results and wrote the manuscript. All authors read and approved the final manuscript. SM and AG checked and approved the authenticity of the raw data.

Ethics approval and consent to participate

Tissue and data collections and analysis were approved by, performed following and in agreement with the criteria of the Ethical Committee of the Azienda Ospedaliero-Universitaria di Careggi (Florence, Italy; no. 0028114). All experiments on animal models were performed following the guidance of the use of laboratory animals and approved by the appointed authority under Italian law (Ministry of Health, Rome, Italy; no. 853/2015-PR).

Patient consent for publication

Not applicable.

Competing interests

The authors declare that they have no competing interests.

References

- Bray F, Ferlay J, Soerjomataram I, Siegel RL, Torre LA and Jemal A: Global cancer statistics 2018: GLOBOCAN estimates of incidence and mortality worldwide for 36 cancers in 185 countries. *CA Cancer J Clin* 68: 394-424, 2018.
- Polvani S, Tarocchi M, Tempesti S, Bencini L and Galli A: Peroxisome proliferator activated receptors at the crossroad of obesity, diabetes, and pancreatic cancer. *World J Gastroenterol* 22: 2441-2459, 2016.
- Siegel RL, Miller KD and Jemal A: Cancer statistics, 2018. *CA Cancer J Clin* 68: 7-30, 2018.
- Guerra F, Guaragnella N, Arbini AA, Bucci C, Giannattasio S and Moro L: Mitochondrial dysfunction: A novel potential driver of epithelial-to-mesenchymal transition in cancer. *Front Oncol* 7: 295, 2017.
- Ceni E, Mello T, Polvani S, Vasseur-Cognet M, Tarocchi M, Tempesti S, Cavalieri D, Beltrame L, Marroncini G, Pinzani M, *et al*: The orphan nuclear receptor COUP-TFII coordinates hypoxia-independent proangiogenic responses in hepatic stellate cells. *J Hepatol* 66: 754-764, 2017.
- Chen X, Qin J, Cheng CM, Tsai MJ and Tsai SY: COUP-TFII is a major regulator of cell cycle and notch signaling pathways. *Mol Endocrinol* 26: 1268-1277, 2012.
- Davis RB, Curtis CD and Griffin CT: BRG1 promotes COUP-TFII expression and venous specification during embryonic vascular. *Development* 140: 1272-1281, 2013.
- Naka H, Nakamura S, Shimazaki T and Okano H: Requirement for COUP-TFI and II in the temporal specification of neural stem cells in CNS development. *Nat Neurosci* 11: 1014-1023, 2008.
- Okamura M, Kudo H, Wakabayashi K, Tanaka T, Nonaka A, Uchida A, Tsutsumi S, Sakakibara I, Naito M, Osborne TF, *et al*: COUP-TFII acts downstream of Wnt/beta-catenin signal to silence PPARgamma gene expression and repress adipogenesis. *Proc Natl Acad Sci USA* 106: 5819-5824, 2009.
- Rosa A and Brivanlou AH: A regulatory circuitry comprised of miR-302 and the transcription factors OCT4 and NR2F2 regulates human embryonic stem cell differentiation. *EMBO J* 30: 237-248, 2011.
- Scroyen I, Bauters D, Vranckx C and Lijnen HR: The anti-adipogenic potential of COUP-TFII is mediated by downregulation of the notch target gene *hey1*. *PLoS One* 10: e0145608, 2015.
- Bao Y, Gu D, Feng W, Sun X, Wang X, Zhang X, Shi Q, Cui G, Yu H, Tang C and Deng A: COUP-TFII regulates metastasis of colorectal adenocarcinoma cells by modulating Snail1. *Br J Cancer* 111: 933-943, 2014.
- Boudot A, Kerdivel G, Lecomte S, Flouriot G, Desille M, Godey F, Leveque J, Tas P, Le Dréan Y and Pakdel F: COUP-TFI modifies CXCL12 and CXCR4 expression by activating EGF signaling and stimulates breast cancer cell migration. *BMC Cancer* 14: 407, 2014.
- Qin J, Wu SP, Creighton CJ, Dai F, Xie X, Cheng CM, Frolov A, Ayala G, Lin X, Feng XH, *et al*: COUP-TFII inhibits TGF- β -induced growth barrier to promote prostate tumorigenesis. *Nature* 493: 236-240, 2013.
- Qin J, Tsai SY and Tsai MJ: The critical roles of COUP-TFII in tumor progression and metastasis. *Cell Biosci* 4: 58, 2014.
- Xu M, Qin J, Tsai SY and Tsai MJ: The role of the orphan nuclear receptor COUP-TFII in tumorigenesis. *Acta Pharmacol Sin* 36: 32-36, 2015.
- Polvani S, Pepe S, Milani S and Galli A: COUP-TFII in health and disease. *Cells* 9: 101, 2019.
- Polvani S, Tarocchi M, Tempesti S, Mello T, Ceni E, Buccoliero F, D'Amico M, Boddi V, Farsi M, Nesi S, *et al*: COUP-TFII in pancreatic adenocarcinoma: Clinical implication for patient survival and tumor progression. *Int J Cancer* 134: 1648-1658, 2014.
- Lin FJ, Qin J, Tang K, Tsai SY and Tsai MJ: Coup d'Etat: An orphan takes control. *Endocr Rev* 32: 404-421, 2011.
- Yamazaki T, Suehiro JI, Miyazaki H, Minami T, Kodama T, Miyazono K and Watabe T: The COUP-TFII variant lacking a DNA-binding domain inhibits the activation of the Cyp7a1 promoter through physical interaction with COUP-TFII. *Biochem J* 452: 345-357, 2013.
- Guasti L, Crociani O, Redaelli E, Pillozzi S, Polvani S, Masselli V, Mello T, Galli A, Amedei A, Wymore RS, *et al*: Identification of a posttranslational mechanism for the regulation of hERG1 K⁺ channel expression and hERG1 current density in tumor cells. *Mol Cell Biol* 28: 5043-5060, 2008.
- Galli A, Ceni E, Mello T, Polvani S, Tarocchi M, Buccoliero F, Lisi F, Cioni L, Ottanelli V, Foresta V, *et al*: Thiazolidinediones inhibit hepatocarcinogenesis in hepatitis B virus-transgenic mice by peroxisome proliferator-activated receptor gamma-independent regulation of nucleophosmin. *Hepatology* 52: 493-505, 2010.
- Bindea G, Mlecnik B, Hackl H, Charoentong P, Tosolini M, Kirilovsky A, Fridman WH, Pagès F, Trajanoski Z and Galon J: ClueGO: A cytoscape plug-in to decipher functionally grouped gene ontology and pathway annotation networks. *Bioinformatics* 25: 1091-1093, 2009.
- Polvani S, Calamante M, Foresta V, Ceni E, Mordini A, Quattrone A, D'Amico M, Luchinat C, Bertini I and Galli A: Acycloguanosyl 5'-thymidyltriphosphate, a thymidine analogue prodrug activated by telomerase, reduces pancreatic tumor growth in mice. *Gastroenterology* 140: 709-720.e9, 2011.
- Lassman AB, Roberts-Rapp L, Sokolova I, Song M, Pestova E, Kular R, Mullen C, Zha Z, Lu X, Gomez E *et al*: Comparison of biomarker assays for EGFR: Implications for precision medicine in patients with glioblastoma. *Clin Cancer Res* 25: 3259-3265, 2019.
- Hennig R, Ventura J, Segersvard R, Ward E, Ding XZ, Rao SM, Jovanovic BD, Iwamura T, Talamonti MS, Bell RH Jr and Adrian TE: LY293111 improves efficacy of gemcitabine therapy on pancreatic cancer in a fluorescent orthotopic model in athymic mice. *Neoplasia* 7: 417-425, 2005.

27. National Research Council (US) Committee for the Update of the Guide for the Care and Use of Laboratory Animals: Guide for the care and use of laboratory animals. 8th edition. National Academies Press (US), Washington, DC, 2011. <https://www.ncbi.nlm.nih.gov/books/NBK54050/> doi: 10.17226/12910.
28. Fernandez-Rachubinski F and Fliegel L: COUP-TFI and COUP-TFII regulate expression of the NHE through a nuclear hormone responsive element with enhancer activity. *Eur J Biochem* 268: 620-634, 2001.
29. Wu SP, Yu CT, Tsai SY and Tsai MJ: Choose your destiny: Make a cell fate decision with COUP-TFII. *J Steroid Biochem Mol Biol* 157: 7-12, 2016.
30. Herreros-Villanueva M, Zhang JS, Koenig A, Abel EV, Smyrk TC, Bamlet WR, de Narvajas AAM, Gomez TS, Simeone DM, Bujanda L and Billadeau DD: SOX2 promotes dedifferentiation and imparts stem cell-like features to pancreatic cancer cells. *Oncogenesis* 2: e61, 2013.
31. Hartel M, Narla G, Wente MN, Giese NA, Martignoni ME, Martignetti JA, Friess H and Friedman SL: Increased alternative splicing of the KLF6 tumour suppressor gene correlates with prognosis and tumour grade in patients with pancreatic cancer. *Eur J Cancer* 44: 1895-1903, 2008.
32. Ganguly K, Krishn SR, Rachagani S, Jahan R, Shah A, Nallasamy P, Rauth S, Atri P, Cox JL, Pothuraju R, *et al*: Secretory Mucin 5AC promotes neoplastic progression by augmenting KLF4-mediated pancreatic cancer cell stemness. *Cancer Res* 81: 91-102, 2021.
33. Shi M, Cui J, Du J, Wei D, Jia Z, Zhang J, Zhu Z, Gao Y and Xie K: A novel KLF4/LDHA signaling pathway regulates aerobic glycolysis in and progression of pancreatic cancer. *Clin Cancer Res* 20: 4370-4380, 2014.
34. Sedgwick AE, Clancy JW, Olivia Balmert M and D'Souza-Schorey C: Extracellular microvesicles and invadopodia mediate non-overlapping modes of tumor cell invasion. *Sci Rep* 5: 14748, 2015.
35. Čermák V, Gandalovičová A, Merta L, Harant K, Rösel D and Brábek J: High-throughput transcriptomic and proteomic profiling of mesenchymal-amoeboid transition in 3D collagen. *Sci Data* 7: 160, 2020.
36. Polizio AH, Chinchilla P, Chen X, Kim S, Manning DR and Riobo NA: Heterotrimeric Gi proteins link Hedgehog signaling to activation of Rho small GTPases to promote fibroblast migration. *J Biol Chem* 286: 19589-19596, 2011.
37. Di Magno L, Basile A, Coni S, Manni S, Sdruscia G, D'Amico D, Antonucci L, Infante P, De Smaele E, Cucchi D, *et al*: The energy sensor AMPK regulates hedgehog signaling in human cells through a unique Gli1 metabolic checkpoint. *Oncotarget* 7: 9538-9549, 2016.
38. Polvani S, Tarocchi M, Tempesti S and Galli A: Nuclear receptors and pathogenesis of pancreatic cancer. *World J Gastroenterol* 20: 12062-12081, 2014.
39. Sato M, Matsumoto M, Saiki Y, Alam M, Nishizawa H, Rokugo M, Brydun A, Yamada S, Kaneko MK, Funayama R, *et al*: BACH1 promotes pancreatic cancer metastasis by repressing epithelial genes and enhancing epithelial-mesenchymal transition. *Cancer Res* 80: 1279-1292, 2020.
40. Polvani S, Tarocchi M and Galli A: PPAR γ and oxidative stress: Con(β) catenating NRF2 and FOXO. *PPAR Res* 2012: 641087, 2012.
41. Lizcano JM and Alessi DR: The insulin signalling pathway. *Curr Biol* 12: R236-R238, 2002.
42. Santo EE, Stroeken P, Sluis PV, Koster J, Versteeg R and Westerhout EM: FOXO3a is a major target of inactivation by PI3K/AKT signaling in aggressive neuroblastoma. *Cancer Res* 73: 2189-2198, 2013.
43. McCubrey JA, Steelman LS, Bertrand FE, Davis NM, Abrams SL, Montalto G, D'Assoro AB, Libra M, Nicoletti F, Maestro R, *et al*: Multifaceted roles of GSK-3 and Wnt/ β -catenin in hematopoiesis and leukemogenesis: Opportunities for therapeutic intervention. *Leukemia* 28: 15-33, 2014.
44. Kim JG, Kim MJ, Choi WJ, Moon MY, Kim HJ, Lee JY, Kim J, Kim SC, Kang SG, Seo GY, *et al*: Wnt3A induces GSK-3 β Phosphorylation and β -catenin accumulation through RhoA/ROCK. *J Cellu Physiol* 232: 1104-1113, 2017.
45. Chou CC, Lee KH, Lai IL, Wang D, Mo X, Kulp SK, Shapiro CL and Chen CS: AMPK reverses the mesenchymal phenotype of cancer cells by targeting the Akt-MDM2-Foxo3a signaling axis. *Cancer Res* 74: 4783-4795, 2014.
46. Lim JK and Leprévier G: The impact of oncogenic RAS on redox balance and implications for cancer development. *Cell Deat Dis* 10: 955, 2019.
47. Teperino R, Amann S, Bayer M, McGee SL, Loipetzberger A, Connor T, Jaeger C, Kammerer B, Winter L, Wiche G, *et al*: Hedgehog partial agonism drives warburg-like metabolism in muscle and brown fat. *Cell* 151: 414-426, 2012.
48. Faget DV, Ren Q and Stewart SA: Unmasking senescence: Context-dependent effects of SASP in cancer. *Nature Rev Cancer* 19: 439-453, 2019.
49. Awasthi N, Mikels-Vigdal AJ, Stefanutti E, Schwarz MA, Monahan S, Smith V and Schwarz RE: Therapeutic efficacy of anti-MMP9 antibody in combination with nab-paclitaxel-based chemotherapy in pre-clinical models of pancreatic cancer. *J Cell Mol Med* 23: 3878-3887, 2019.
50. Xie J, Zhou X, Wang R, Zhao J, Tang J, Zhang Q, Du Y and Pang Y: Identification of potential diagnostic biomarkers in MMPs for pancreatic carcinoma. *Medicine (Baltimore)* 100: e26135, 2021.
51. Grünwald B, Vandooren J, Gerg M, Ahomaa K, Hunger A, Berchtold S, Akbareian S, Schaten S, Knolle P, Edwards DR, *et al*: Systemic ablation of MMP-9 triggers invasive growth and metastasis of pancreatic cancer via deregulation of IL6 expression in the bone marrow. *Mol Cancer Res* 14: 1147-1158, 2016.
52. Wang L, Cheng CM, Qin J, Xu M, Kao CY, Shi J, You E, Gong W, Rosa LP, Chase P, *et al*: Small-molecule inhibitor targeting orphan nuclear receptor COUP-TFII for prostate cancer treatment. *Sci Adv* 6: eaaz8031, 2020.



This work is licensed under a Creative Commons Attribution-NonCommercial-NoDerivatives 4.0 International (CC BY-NC-ND 4.0) License.